



Brazilian Journal of Physics

ISSN: 0103-9733

luizno.bjp@gmail.com

Sociedade Brasileira de Física
Brasil

García-Sánchez, Eduardo; Mendoza-Huizar, Luis H.; Ramírez-García, Uriel; Sustaita, Ireri
A.; Alvarado, Francisco

Analysis of the Influence of the Molecular Volume to Predict Experimental Pressure-
Temperature Behavior in the Isotropic-Nematic Phase Transition of PAP, 5CB, MBBA and
EBBA

Brazilian Journal of Physics, vol. 45, núm. 2, abril, 2015, pp. 258-263

Sociedade Brasileira de Física
São Paulo, Brasil

Available in: <http://www.redalyc.org/articulo.oa?id=46438835011>

- How to cite
- Complete issue
- More information about this article
- Journal's homepage in [redalyc.org](http://www.redalyc.org)

[redalyc.org](http://www.redalyc.org)

Scientific Information System

Network of Scientific Journals from Latin America, the Caribbean, Spain and Portugal

Non-profit academic project, developed under the open access initiative

Analysis of the Influence of the Molecular Volume to Predict Experimental Pressure-Temperature Behavior in the Isotropic-Nematic Phase Transition of PAP, 5CB, MBBA and EBBA

Eduardo García-Sánchez · Luis H. Mendoza-Huizar ·
Uriel Ramírez-García · Ileri A. Sustaita ·
Francisco Alvarado

Received: 27 October 2014 / Published online: 14 January 2015
© Sociedade Brasileira de Física 2015

Abstract In this work, we have analyzed the experimental pressure-temperature behavior at the isotropic-nematic phase transition of the liquid crystals PAP, 5CB, MBBA, and EBBA at 1 atm by using the HERSW Convex Peg model in conjunction with the IPCM model. We have calculated the molecular volume values for the hard and attractive cores from theoretical quantum calculations at the PM3, PM6, B3LYP/6-311++G(d,p)/PM6, and M06/6-311++G(d,p)/PM6 levels of theory. The results suggest that the best theoretical prediction of the experimental pressure-temperature behavior is obtained when the molecular volume is evaluated at the DFT level.

Keywords Phase transitions · Isotropic-nematic · Convex peg

1 Introduction

A liquid crystal (LC) is an aggregation state whose properties are intermediate between a crystalline solid and an amorphous liquid [1]. It is important to mention that under appropriate conditions, the axis of the molecules in an LC can be aligned in a particular direction. Thus, if one modifies such direction, a variety of arrangements and phase transitions may be obtained.

Moreover, these LC phase transitions may be induced by electric or magnetic fields [2–4]. These phase transitions have technological importance because they can be used to modify the optical properties of LCs without changing its composition [5]. Therefore, the development of predictive theories that allow the correct prediction of LC phase transitions is of great fundamental and applied interest.

Specifically, PAP (4-4'-bis (ethyloxy) azoxybenzene), 5CB (4-pentyl-4'-cyanobiphenyl), MBBA (4-methoxybenzilidene-4'-butylaniline), and EBBA (4-ethoxybenzilidene-4'-butylaniline) liquid crystals have attracted a great interest in view of their potential applications in scientific and technological fields. These liquid crystals exhibit isotropic-nematic (I-N) phase transitions which can be used in the fabrication of liquid crystal displays (LCD) [6–10]. However, the presence of heating lamps in such LCD may cause an increment on the temperature, around of 50 °C. These operating conditions may modify the optical properties of these LCs [11]. Also, in the electronic industry, these LCs can be used as temperature indicators to locate the precise site where an electronic component fails due to overheating, short circuit, or even a bad design. If one considers that in such place there will be an increment of the current density, then a hot spot will be located in this site. Thus, the sensibility of LCs to temperature gradients allows to identify, through a change in their coloration, the site of the fail by mean of the technique so called liquid crystal thermography (LCT) [12, 13]. In addition, the PAP, MBBA, and EBBA nematic liquid crystals can be used as lubricants because they are able to diminish the friction between surfaces [14]. For example, the viscosity of MBBA exhibits a lower value in the nematic phase in comparison to the isotropic phase [15]. Also, in this LC, the nematic ordering and low friction coefficient values are maintained when the temperature is above the

E. García-Sánchez (✉) · U. Ramírez-García · I. A. Sustaita ·
F. Alvarado
Unidad Académica de Ingeniería Eléctrica, Universidad Autónoma
de Zacatecas, Av. Ramón López Velarde No. 801, Zacatecas,
México 98600
e-mail: eduardogarciasanchez@gmail.com

L. H. Mendoza-Huizar
Área Académica de Química, Universidad Autónoma del Estado de
Hidalgo, Unidad Universitaria, Km. 4.5, Carretera
Pachuca-Tulancingo, Mineral de la Reforma, Hidalgo, México

isotropic-nematic transition temperature. Furthermore, it is important to consider that the temperature of the isotropic-nematic phase transition varies with the pressure, which is related to changes in the density value [15, 16].

The above mentioned suggests a wide application of the LCs as a function of the temperature of the system [11]. Considering these facts, it is not surprising that many efforts are being focused on developing thermodynamic models, which may predict adequately their experimental pressure-temperature behavior [10]. However, as far as we know, a detailed knowledge about the behavior of the isotropic and transition regions of PAP, 5CB, MBBA, and EBBA at 1 atm, as a function of the temperature, is missing [13]. Here, it is important to mention that a good knowledge of the limit values of pressure and temperature would allow us to identify the values of P-T where the nematic order is obtained.

Onsager [3] demonstrated that repulsive interactions are important in the prediction of the isotropic-nematic (I-N) phase transition. On the other hand, Maier and Saupe [17] proposed a model in which this I-N phase transition is driven by anisotropy in the long range attractive forces. Initially, Kimura [18] combined Onsager's hard-rod model with anisotropic dispersion forces. Some further progress has been made in understanding the effect of hard-core [19–23], generalized attractive potential [24–37], dipolar [38–43], or chiral [44–46] interaction on the stability of various LC phases.

In our research group, it has been observed that the prediction of the experimental pressure-temperature behavior of PAP, 5CB, MBBA, and EBBA may be improved when the molecular volume (V_m) is evaluated through quantum calculations, and this value is used in the thermodynamic predictions [24–29]. Bearing in mind the importance of V_m in this kind of studies, García-Sánchez et al. [26] predicted the phase diagram and the I-N phase transition for p-azoxyanisole (PAA), 5CB, and 4-4'-bis (heptiloxo) azoxybenzene (HOAOB). In this prediction, the estimation of the V_m and $\lambda=a/b$ (the convex peg model comprising a convex hard core with semi-axis ratio $a:b$ surrounded by a spherical square-well of depth ε and range λb) was carried out by using semiempirical and isodensity polarized continuous model (IPCM) calculations [47]. Then, the V_m obtained was mapped into a hard ellipsoid revolution volume of a convex peg molecule. The results were in good agreement to the experimental pressure-temperature behavior reported for I-N transition [10]. In other work, García-Sánchez et al. [29] evaluated the effect of the potential range in the pressure-temperature behavior of PAP, 5CB, MBBA, and EBBA. In this work, it was found that the prediction of the experimental data is improved when both optimized parameters, V_m and the potential range, are considered. In a different context, González-Cabrera et al. [28] analyzed the experimental pressure-temperature behavior in the PAA I-N phase transition at 1 atm employing different

convex peg models (HERSW, HERSWS [24] and HERSWE). In that work, a/b and V_m parameters were obtained in the framework of the density functional theory (DFT) and the IPCM method [47]. Additionally, the effect of varying the geometry of the attractive contribution in the convex peg model was analyzed, in order to predict the experimental pressure-temperature behavior. The results suggested that the convex peg model HERSW predicts quantitatively the experimental behavior for PAA. Moreover, in these studies, the value of V_m was identified as a key parameter during the prediction of the PAA I-N phase transition [24–29]. Here, it is important to mention that the V_m calculated in previous works by García-Sánchez et al. [24–29] was carried out considering an isolated molecule. Thus, in the present work, we have analyzed the influence of the intermolecular interactions in the determination of the molecular volume value of PAP, 5CB, MBBA, and EBBA and their effect on the prediction of the experimental pressure-temperature behavior during the I-N phase transitions of these LCs. We consider that this kind of study is important to identify the parameters that direct the liquid crystal behavior.

2 Theory

In this work, we have used the perturbation theory and the convex peg HERSW model proposed by González-Cabrera et al. [28] which is expressed as

$$\frac{A}{NkT} = \frac{A_{\text{ideal}}}{NkT} + \frac{A_{\Omega}}{NkT} + \frac{A_{\text{excess}}}{NkT} + \frac{A_{\text{attractive}}}{NkT}, \quad (1)$$

where k is the Boltzmann's constant, T is the temperature, V is the volume, N is the number of molecules, A_{ideal} is the ideal contribution to the free energy, A_{Ω} is a contribution to the free energy coming from the loss of entropy due to the orientational order, A_{excess} is the free energy of the reference fluid and $A_{\text{attractive}}$ is the attractive contribution of free energy. The ideal contribution is given by

$$\frac{A_{\text{ideal}}}{NkT} = \ln(\rho\Delta^3) - 1. \quad (2)$$

In this expression, Δ is the Broglie's mean thermal wavelength and ρ is the density ($\rho=N/V$). The orientational term of free energy is given by the Onsager's expression [3]:

$$\frac{A_{\Omega}}{NkT} = \int f(\Omega) \ln[f(\Omega)] d\Omega, \quad (3)$$

where $f(\Omega)$ is the single particle orientational distribution function for a solid angle Ω . In the isotropic phase, $f(\Omega)$ is

uniform, whereas for a nematic phase, $f(\Omega)$ is a no uniform function. The hard core or excess free energy is given by

$$\frac{A_{\text{excess}}}{NkT} = \frac{\langle V_{\text{ex}}^{\text{HC}}(\Omega_1, \Omega_2) \rangle}{8V_0} \left[\frac{4\eta - 3\eta^2}{(1 - \eta)^2} \right]. \quad (4)$$

In this equation, $V_0 = V_m$ is the volume of the hard core, $\eta = \rho V_0$ is the packing fraction, $V_{\text{ex}}^{\text{HC}}(\Omega_1, \Omega_2)$ is the volume excluded to one particle with orientation given by Ω_2 due to the presence of another particle oriented along Ω_1 , and the angular brackets represent a weighted average over the molecular orientations.

The attractive contribution to the free energy is given by

$$\frac{A_{\text{attractive}}}{NkT} = -\frac{\rho}{2} \left[e^{\frac{1}{T^*}} - 1 \right] \left[\frac{\langle V_{\text{ex}}^{\lambda}(\Omega_1, \Omega_2) \rangle}{\langle V_{\text{ex}}^{\text{HC}}(\Omega_1, \Omega_2) \rangle} - 1 \right] \langle V_{\text{ex}}^{\text{HC}}(\Omega_1, \Omega_2) \rangle, \quad (5)$$

where ε is the square-well depth, λ is the square-well range, $T^* = kT/\varepsilon$ is the reduced temperature and $\langle V_{\text{ex}}^{\lambda}(\Omega_1, \Omega_2) \rangle$ is the excluded volume of two attractive cores with arbitrary

orientations Ω_1 and Ω_2 . On the other hand, it is possible to consider that

$$\frac{\langle V_{\text{ex}}^{\lambda}(\Omega_1, \Omega_2) \rangle}{\langle V_{\text{ex}}^{\text{HC}}(\Omega_1, \Omega_2) \rangle} = \frac{V_0^{\text{attractive}}}{V_0^{\text{HC}}} = \left(\frac{b_{\lambda}}{b} \right)^2. \quad (6)$$

Here, $V_0^{\text{HC}} = V_0$ and $V_0^{\text{attractive}}$ is the volume of the attractive core region, respectively, and b_{λ} is the semi-minor axis of the attractive ellipsoidal shaped SW range [28].

3 Methodology

In general, to evaluate the free energy, the functional must be minimized with respect to $f(\Omega)$. In the isotropic phase, $f(\Omega)$ takes the value 1 because the orientational term of the free energy (Eq. 3) gives zero for this phase, substituting this into the full expression for the free energy (Eq. 1), the necessary integrals can be evaluated and a closed expression for the isotropic free energy is obtained. In the case of a nematic phase, we have to consider the Eq. 1 as a free energy

Table 1 Molecular volume obtained for PAP, 5CB, EBBA, and MBBA at different levels of theory

System	Level of theory	Individual molecular volume 0.08 electrons/Å ³	Molecular volume 0.002 electrons/Å ³	a/b	<i>a</i> / <i>b</i> _λ	<i>b</i> _λ / <i>b</i>	
5CB	PM3	80.08 [25,28]	326.14	3.7	1.834	2.018	
				3.8	1.883	2.018	
5CB	PM6	80.25	327.53	3.7	1.832	2.020	
				3.8	1.881	2.020	
5CB	B3LYP/6-311++G(d,p)	80.19	257.60	3.7	2.065	1.792	
				3.8	2.121	1.792	
(5CB) ₆	B3LYP/6-311++G(d,p)//PM6	76.37	305.54	3.7	1.850	2.000	
		M06/6-311++G(d,p)//PM6	76.37	305.54	3.7	1.850	2.000
					3.8	1.900	2.000
EBBA	PM3	89.07 [25]	371.60	3.0	1.468	2.043	
EBBA	PM6	92.42	396.09	3.0	1.449	2.070	
EBBA	B3LYP/6-311++G(d,p)	94.55	305.84	3.0	1.668	1.799	
(EBBA) ₅	B3LYP/6-311++G(d,p)//PM6	96.14	358.93	3.0	0.804	3.733	
		M06/6-311++G(d,p)//PM6	96.14	358.93	3.0	0.804	3.733
MBBA	PM3	89.15 [28]	371.90	3.0	1.469	2.042	
MBBA	PM6	82.85	343.14	3.0	1.474	2.035	
MBBA	B3LYP/6-311++G(d,p)	82.82	341.48	3.0	1.477	2.031	
(MBBA) ₆	B3LYP/6-311++G(d,p)//PM6	81.52	330.48	3.0	1.490	2.013	
		M06/6-311++G(d,p)//PM6	81.52	330.48	3.0	1.490	2.013
PAP	PM3	81.05	268.04	3.6	1.979	1.819	
PAP	PM6	81.17	331.30	3.6	1.782	2.020	
PAP	B3LYP/6-311++G(d,p)	81.26	268.61	3.6	1.980	1.818	
(PAP) ₆	B3LYP/6-311++G(d,p)//PM6	83.95	320.91	3.6	1.841	1.955	
		M06/6-311++G(d,p)//PM6	83.95	320.91	3.6	1.841	1.955

functional of $f(\Omega)$, which must be minimized with respect to this function. In this work, we have used a numerical minimization through the Onsager's trial function:

$$f(\theta) = \frac{\alpha \cosh(\alpha \cos \theta)}{\sinh \alpha}, \quad (7)$$

where α is a variable parameter. Normally, in this process, a temperature is chosen and the free energy is minimized over a range of η . The minimized values for α are fitted to a polynomial in η and substituted back into the free energy for the nematic phase expression.

Once we have obtained the free energies for the isotropic and nematic phases, the reduced pressure P and chemical potential μ can be calculated by using the usual thermodynamic relationship, given by

$$\frac{PV_0}{kT} = \eta \left(1 + \eta \frac{\partial(A(\alpha) - A^{\text{ideal}})}{\partial \eta} \right), \quad (8)$$

and

$$\frac{\mu}{kT} = \ln(\eta) + \sigma(\alpha) + \frac{(A(\alpha) - A^{\text{ideal}})}{NkT} + \eta \left[\frac{\partial(A(\alpha) - A^{\text{ideal}})}{\partial \eta} \right], \quad (9)$$

where $\sigma(\alpha)$ is obtained by substituting the trial function into the expression (3) and integrating. The isotropic-nematic phase transition is then evaluated by ensuring, at a fixed temperature, that the chemical potential and pressure of each phase are the same. In the expressions above mentioned, note that the value of the molecular volume is an important factor to obtain a good experimental prediction of the isotropic-nematic phase transition. In previous works, we found that the molecular volume may be related to the space occupied by a molecule under its minimal energy geometry configuration. Thus, the occupied volume depends on the size of the atoms forming the molecule where such size is a direct function of the molecular electronic density. It has been reported that the

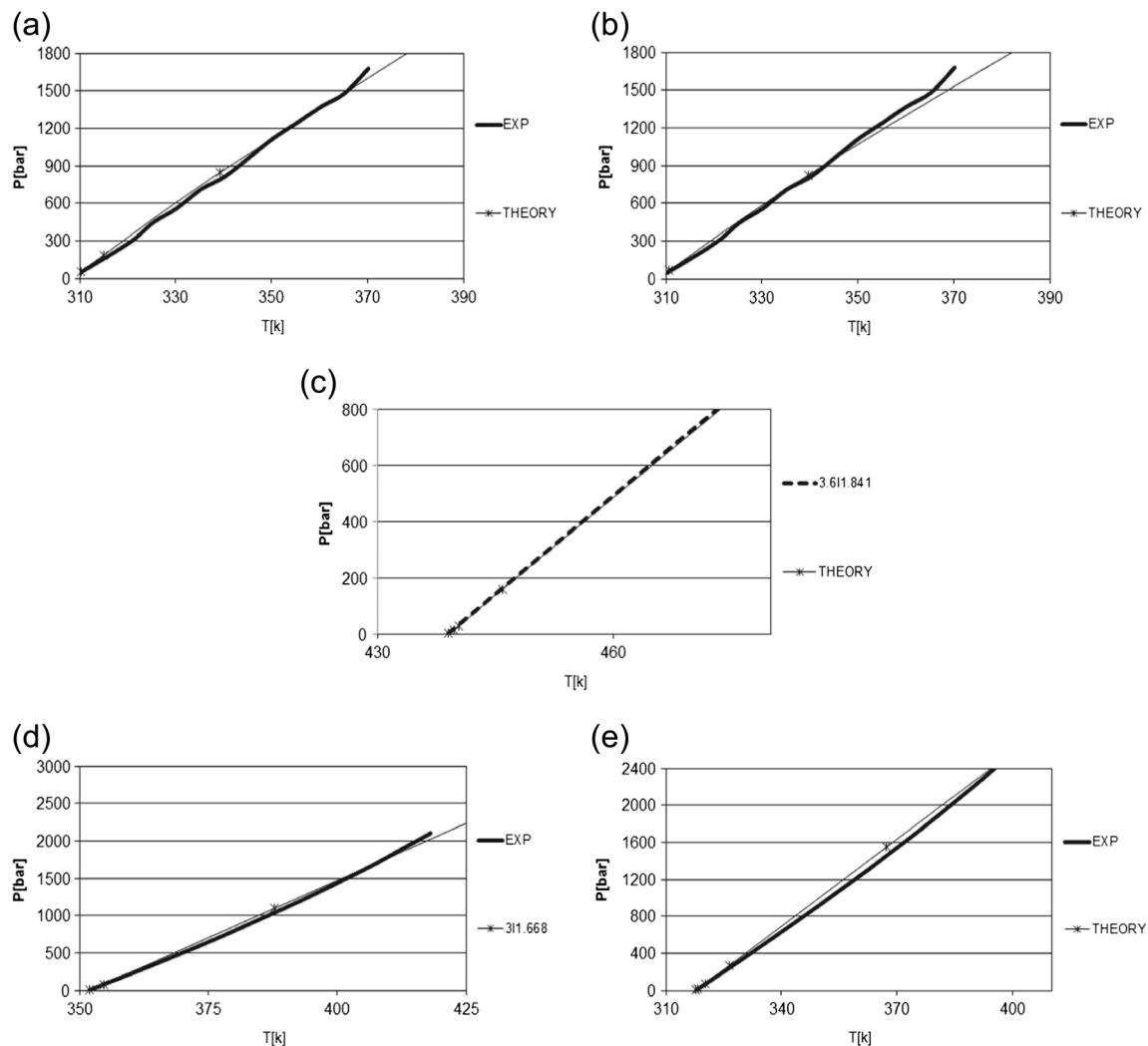


Fig. 1 Comparison among theoretical prediction of HERSW model and experimental data of pressure-temperature behavior in the I-N phase transition at 1 atm [9] of (a) 5CB with $a/b=3.7$, (b) 5CB with $a/b=3.8$, (c) PAP with $a/b=3.6$, (d) EBBA with $a/b=3.0$, and (e) MBBA with $a/b=3.0$

value of the electronic density may be evaluated employing the accepted theories of the quantum chemistry [24, 28].

Also, in the present work, we have analyzed the influence of the intermolecular interactions caused by the presence of other molecules on the individual molecular volume. The systems (PAP)₆, (5CB)₆, (EBBA)₅, and (MBBA)₆ were optimized employing the semiempirical PM6 method [48, 49]. The geometries optimized at the PM6 level were used to calculate the value of the molecular volume occupied by the electronic density at 0.08 and 0.002 electrons/Å³, and it was related with the molecular volume of the hard and attractive cores for each LC considered in the present work. To analyze the influence of the electronic correlation in the volume occupied by electrons, we carried out quantum calculations at the B3LYP/6-311++G(d,p)/PM6 and M06/6-311++G(d, p)//PM6 levels. In all the calculations, we used the IPCM model [50–52], Q-chem ver. 3.0 [53] and Gaussian 09 [54] packages.

4 Results and Discussion

Table 1 reports the values of the molecular volumes for the hard and attractive cores (0.08 and 0.002 electrons/Å³, respectively) obtained at different levels of theory. Note, that the molecular volume for the attractive core of the isolated PAP, 5CB, MBBA, and EBBA molecules are greater than when they are part of a cluster. This fact may be explained in terms of the intermolecular interactions generated when two or more molecules are interacting. Thus, the presence of functional groups in these LC may favor the apparition of attractive or repulsive interactions, which will cause the increment or decrement of the molecular volume value. Table 1 reports the values of a/b [25, 28] for 5CB, PAP, EBBA, and MBBA liquid crystals.

Here, it is important to mention that a traditional hybrid functional as B3LYP is not able to take into account weak interactions which are very important during the interaction of two molecules. In this sense, the functional M06 is able to analyze the effect of these non-covalent interactions [55]. In order to compare the values of the volume enclosed obtained through both functionals, we calculated the value of the volume enclosed by the electronic density at the B3LYP/6-311++G(d,p)/PM6 and M06/6-311++G(d,p)/PM6 levels. Similar values of the volume enclosed by the electronic density were obtained at both levels of theory. This result suggests that the molecular volume is highly dependent on the molecular geometry. Although in this work we have used the PM6 geometry, it is interesting to note that the use of high levels of theory as M06/6-311++G(d,p)/PM6 do not improve appreciably the prediction of the molecular volume based on the electronic density.

Figure 1 shows a comparison of the theoretical values obtained in the present work with the experimental data [10]

reported for 5CB, PAP, EBBA, and MBBA. Observe that the theoretical results, at different levels of theory, closely follow the experimental results. Thus, in Fig. 1, we present only the best prediction for each case. The best prediction is obtained at the DFT level. Specifically, for 5CB with $a/b=3.7$, $a/b_\lambda=2.065$, and $b_\lambda/b=1.792$ (Fig. 1a), for 5CB with $a/b=3.8$, $a/b_\lambda=2.121$, and $b_\lambda/b=1.792$ (Fig. 1b), for PAP with $a/b=3.6$, $a/b_\lambda=1.98$, and $b_\lambda/b=1.818$ (Fig. 1c), for EBBA with $a/b=3.0$, $a/b_\lambda=1.668$, and $b_\lambda/b=1.799$ (Fig. 1d), and finally, for MBBA with $a/b=3.0$, $a/b_\lambda=1.477$, and $b_\lambda/b=2.031$ (Fig. 1e). As observed in Fig. 1, the experimental pressure-temperature behavior is predicted adequately in the I-N phase transition for all cases analyzed in the present work. The above mentioned indicates that the theoretical prediction of the experimental pressure-temperature behavior is improved when the molecular volume is evaluated through quantum calculations. Also, the perturbation theory proposed by González-Cabrera et al. [28], make simpler the expression of the Helmholtz free energy (Eq. 6), because this theory only requires the expression $\langle V_{ex}^{HC}(\Omega_1, \Omega_2) \rangle$ and not $\langle V_{ex}^\lambda(\Omega_1, \Omega_2) \rangle$.

5 Conclusions

In this work, we have analyzed the experimental pressure-temperature behavior at the isotropic-nematic phase transition for PAP, 5CB, MBBA and EBBA at 1 atm by using an extension of the HERSW convex peg model in a perturbation theory to second order. Additionally, we have obtained the values of the molecular volumes for the hard and attractive cores from theoretical quantum calculations at the PM3, PM6, B3LYP/6-311++G(d,p), and M06/6-311++G(d,p) levels considering the presence of intermolecular interactions. In general, we found that the best theoretical predictions for experimental data are obtained at the DFT level.

Acknowledgments EGS and LHMH gratefully acknowledge financial support from the Universidad Autónoma de Zacatecas and from the Universidad Autónoma del Estado de Hidalgo, respectively. LHMH wishes to thank the financial support from CONACYT (project INFR-2014-227999) and National Laboratory for the Characterization of Physicochemical Properties and Molecular Structure, (LACAPFEM) for providing supercomputing time. We are also grateful to the reviewers of the manuscript for valuable suggestions.

References

1. S. Chandrasekhar, *Liquid Crystals*, second edition, Cambridge University Press, pp. 1-16 (1992)
2. L. Onsager, *Ann. N. Y. Acad. Sci.* **51**, 627 (1949)
3. M.P. Allen, G.T. Evans, D. Frenkel, B.M. Mulder, *Adv. Chem. Phys.* **86**, 1 (1993)
4. G.J. Vroege, H.N.W. Lekkerkerker, *Rep. Prog. Phys.* **55**, 1241 (1992)

5. Y.C. Lin, D.O. Duncenco, Y.S. Huang, K. Suenaga, *Nat. Nanotechnol.* **9**, 391 (2014)
6. A. Chanishvili, G. Chilaya, G. Petriashvili, D. Sikharulidze, *Mol. Cryst. Liq. Cryst.* **409**, 209 (2004)
7. A. Chanishvili, G. Chilaya, G. Petriashvili, P.J. Collings, *Phys. Rev. E* **71**, 051705 (2005)
8. M. Johri et al., *Phys.* **76**, 621 (2011)
9. J. Pavlin et al., *Eurasia J. Math. Sci. &Tech. Ed.* **7**, 173 (2011)
10. G.R. Van Hecke, Phase transitions and the effects of pressure, *Thermodynamics, Physical Properties of Liquid Crystals: Nematics*, EMIS Datareviews Series; No. 25, (INSPEC, the Institution of Electrical Engineers, London, United Kingdom), pp 265–276 (2001)
11. O.M. Abdul-Aziz, J.R. Abdul-Karim, A. Mohammed, A.O. Karar, Calculation of refractive index for (MBBA) liquid crystal material at different temperatures. *J Babylon Univ. Pure. Appl. Sci.* **21**(5), 1764–1768 (2013)
12. S. Khandekar, K.S. Wills. *Liquid Crystal Microscopy*, In: *Microelectronic Failures Analysis Desk Reference*, Fourth Ed., EDFAS, pp 739–44 (2002)
13. V.M. Popov, A.S. Klimenko, A.P. Pokanevich, I. Gavriluk, A.P. Pokanevich, *Mikroelektronika* **36**(6), 446 (2007)
14. G. Biresaw, *Tribology and the Liquid-crystalline State: Developed from a Symposium Sponsored by the Division of Colloid and Surface Chemistry at the 198th National Meeting of the American Chemical Society, Miami Beach, Florida, September 10–15. J. Cognard. Lubrication with Liquid Crystal*, Chapter 1, pp 1–47 (1989)
15. E. Kuss, *Mol. Cryst. Liq. Cryst.* **47**, 71 (1978)
16. J. Deschamps, J.P. Martin Trusler, G. Jackson, *J. Chem. Phys. B* **112**, 3918 (2008)
17. W. Maier, A. Saupe, *Z. Naturf.* **13**, 564 (1958)
18. H. Kimura, *J. Physics. Soc. Jpn.* **36**, 1280 (1974)
19. J.D. Parsons, *Phys. Rev. A* **19**, 1225 (1979)
20. S.D. Lee, *J. Chem. Phys.* **87**, 4972 (1987)
21. S.D. Lee, *J. Chem. Phys.* **89**, 7036 (1988)
22. N.F. Carnahan, K.E. Starling, *J. Chem. Phys.* **51**, 635 (1969)
23. L.V. Yelash, T. Kraska, E.A. Muller, N.F. Carnahan, *Phys. Chem. Chem. Phys.* **1**, 4919 (1999)
24. E. García-Sánchez et al., *J. Chem. Phys. A* **106**, 10340 (2002)
25. A. Martínez-Richa, E. García-Sánchez, D.C. Williamson, *Rev. Mex. Ing. Quim.* **2**, 35 (2003)
26. E. García-Sánchez, *Rev. Méx. Fis.* **53**, 179 (2007)
27. E. García-Sánchez, F.J. Martínez, L.H. Mendoza-Huizar, *Información Tecnológica.* **20**, 39 (2009)
28. A.E. González-Cabrera, E. García-Sánchez, L.H. Mendoza-Huizar, *J. Mol. Liq.* **149**, 22 (2009)
29. E. García-Sánchez, J.M. Cervantes-Viramontes, C.H. Castañeda-Ramírez, *Ing. Inv. Tec.* **2**, 157 (2011)
30. M.A. Cotter, *J. Chem. Phys.* **66**, 4710 (1977)
31. W.M. Gelbart, B.A. Baron, *J. Chem. Phys.* **66**, 207 (1977)
32. W.M. Gelbart, B. Barboy, *Acc. Chem. Res.* **13**, 290 (1980)
33. P.G. Bolhuis, A. Stroobants, D. Frenkel, H.N.W. Lekkerkerker, *J. Chem. Phys.* **107**, 1551 (1997)
34. D.C. Williamson, *Mol. Phys.* **95**, 319 (1998)
35. P.I.C. Teixeira, *Mol. Phys.* **96**, 805 (1999)
36. D.C. Williamson, F. Del Rio, *J. Phys. Chem. B* **109**, 4675 (1998)
37. D.C. Williamson, Y. Guevara, *J. Phys. Chem. B* **103**, 7522 (1999)
38. S.C. McGrother, A. Gil-Villegas, G. Jackson, *J. Phys. Condens. Matter* **8**, 9649 (1996)
39. B. Groh, S. Dietrich, *Phys. Rev. E* **55**, 2892 (1997)
40. A. Gil-Villegas, S.C. McGrother, G. Jackson, *Chem. Phys. Lett.* **269**, 441 (1997)
41. S.C. McGrother, A. Gil-Villegas, G. Jackson, *Mol. Phys.* **95**, 657 (1998)
42. S. Varga, I. Szalai, J. Liszi, G. Jackson, *J. Chem. Phys.* **116**, 9107 (2002)
43. D.C. Williamson, N.A. Thacker, S.R. Williamson, *Phys. Rev. E* **71**, 021702 (2005)
44. S. Varga, G. Jackson, *Mol. Phys.* **104**, 3681 (2006)
45. H.H. Wensink, G. Jackson, *J. Chem. Phys.* **130**, 234911 (2009)
46. H.H. Wensink, G. Jackson, *J. Phys.: Condens. Matter* **23**, 194107 (2011)
47. J.B. Foresman et al., *J. Phys. Chem.* **100**, 16098 (1996)
48. J.J.P. Stewart, *J. Comp. Chem.* **10**, 209 (1989)
49. J.J.P. Stewart, *J. Mol. Model.* **13**, 1173 (2007)
50. L. Onsager, *J. Am. Chem. Soc.* **58**, 1486 (1936)
51. S. Miertus, E. Scrocco, J. Tomasi, *Chem. Phys.* **55**, 117 (1981)
52. J. Tomasi, M. Persico, *Chem. Rev.* **94**, 2027 (1994)
53. Y. Shao et al., *Phys. Chem. Chem. Phys.* **8**, 3172 (2006)
54. Gaussian 09, Revision C.01, MJ Frisch et al. Gaussian, Inc., Wallingford CT, 2009.
55. Y. Zhao, D.G. Truhlar, *Theor. Chem. Account.* **120**, 215 (2008)